Electronic Supplementary Information

Charge transport in organic donor-acceptor mixed-stack crystals: the role of nonlocal electron-phonon couplings

Lingyun Zhu[1,*], Hua Geng[2], Yuanping Yi[2,*], Zhixiang Wei[1]

[1] CAS Key Laboratory of Nanosystem and Hierarchircal Fabrication, CAS Center for Excellence in Naoscience, National Center for Nanoscience and Technology, Beijing 100190, China

[2] Beijing National Laboratory for Molecular Sciences, CAS Key Laboratory of Organic Solids, Institute of Chemistry, Chinese Academy of Sciences, Beijing 100190, China

*Corresponding authors. E-mails: zhuly@nanoctr.cn (LZ); ypyi@iccas.ac.cn (YY).

Table S1. Comparison of optimized lattice parameters for the DMQtT-F_4TCNQ crystal based on different force fields.

	Exp.	Dreiding	Deviation	Universal	Deviation	Compass	Deviation
a **(Å)**	10.185	10.294	1.1%	10.923	7.2%	10.118	0.7%
b **(Å)**	10.568	11.122	5.2%	11.040	4.5%	10.726	1.5%
c **(Å)**	6.842	6.671	2.5%	6.387	6.7%	6.740	1.5%
α()	98.920	100.217	1.3%	99.634	0.7%	98.539	0.4%
β()	95.890	97.901	2.1%	102.756	7.2%	99.710	4.0%
γ()	67.240	64.912	3.5%	60.244	10.4%	62.050	7.7%

Table S2. Crystallographic parameters for the unit cells of the investigated mixed-stack crystals (all the crystals belong to the $P\bar{1}$ space group).

	a **(Å)**	***b*** **(Å)**	***c*** **(Å)**	α()	β()	γ()
C_8BTBT-TCNQ	7.1829	7.7361	17.946	86.554	80.529	73.518
C_8BTBT-F_2TCNQ	7.1554	7.8669	17.710	86.350	81.334	72.909
C_8BTBT-F_4TCNQ	7.1030	8.0777	17.592	85.900	82.020	72.443
DMQtT-F_4TCNQ	10.185	10.568	6.842	98.92	95.890	67.240

Table S3. Internal reorganization energy λ (in meV), classical contribution to the internal reorganization energy λ_{cls} (in meV), effective frequency ω_{eff} (in cm^{-1}) and Huang-Rhys factor S_{eff}.

		λ	λ_{cls}	ω_{eff}	S_{eff}
hole	**C_8BTBT**	244	12.6	823.7	1.095
	DMQtT	297	34.0	1046.9	0.999
electron	**TCNQ**	257	6.6	814.5	1.224
	F_4TCNQ	256	6.6	814.5	1.223

Table S4. Effective super-exchange electronic couplings calculated by the Larsson partition method based on the crystal structures optimized by the Dreiding force field.

	Hole	Electron
C_8BTBT-TCNQ	38	-62
C_8BTBT-F_2TCNQ	41	-63
C_8BTBT-F_4TCNQ	46	-65
DMQtT-F_4TCNQ	-124	105

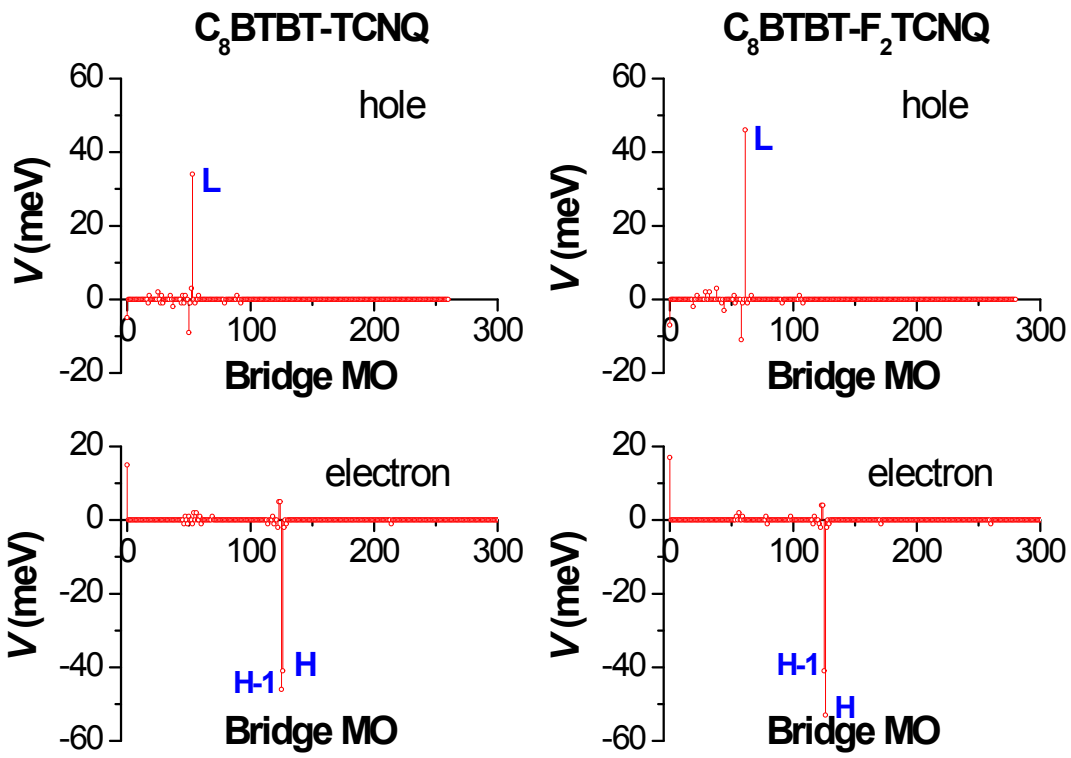

Figure S1. Decomposition of the super-exchange couplings (t^{eff}) for hole [electron] transport into each molecular orbital (MO) of the middle acceptor [donor] bridge for the C_8BTBT-F_4TCNQ and DMQtT-F_4TCNQ systems.

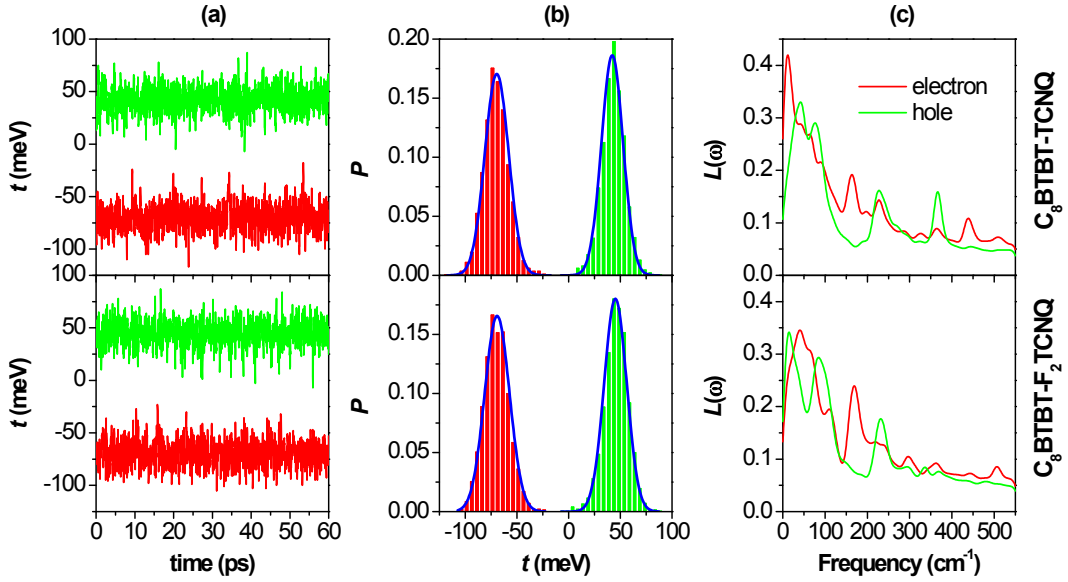

Figure S2. (a) Evolution of transfer integrals with sampling time, (b) Distribution probability of transfer integrals, and (c) Frequency dependence of parameter *L* for the super-exchange transport of the C_8BTBT-TCNQ and C_8BTBT-F_2TCNQ crystals.

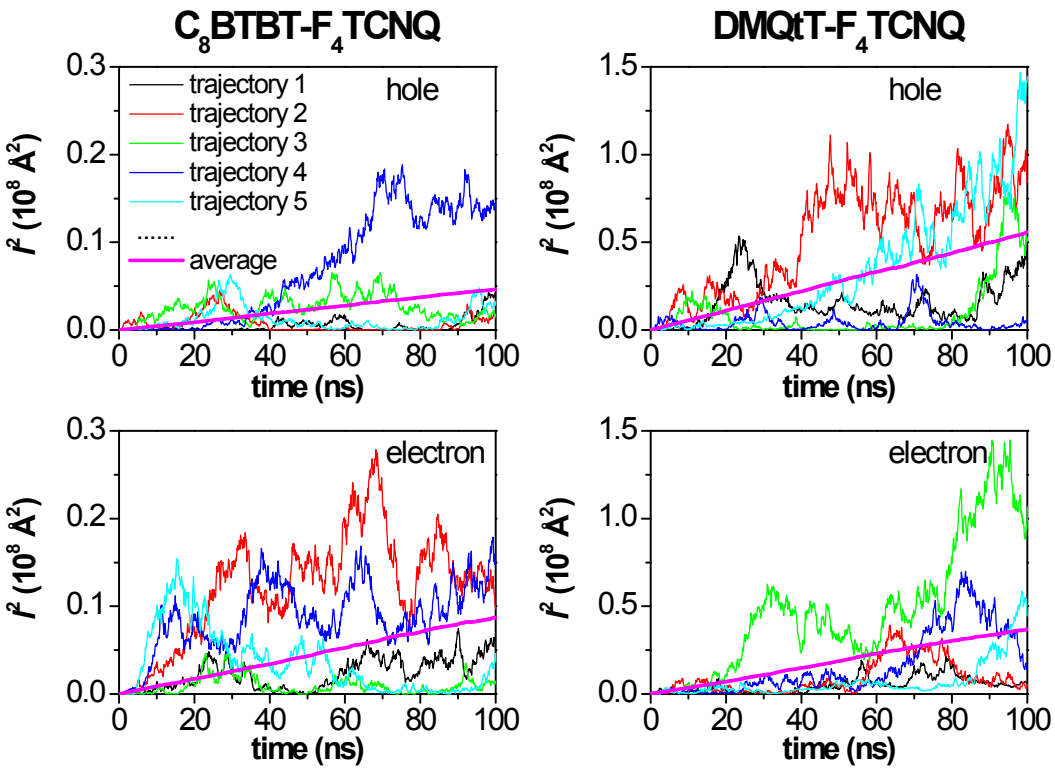

Figure S3. Time evolution of the square displacement of five individual simulations and the mean-square displacement over 2000 simulations which were carried out with dynamic disorder considered and external reorganization energy set to 0.4 eV.